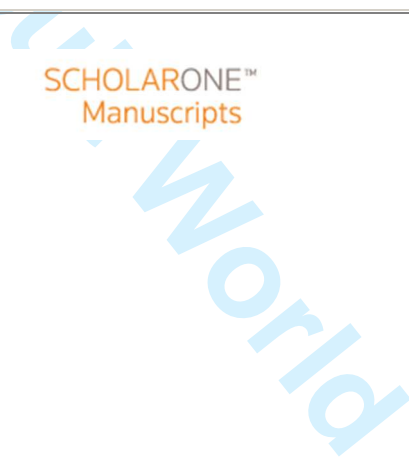




Morphology and acoustic artefacts of copper deposits electroplated using megasonic assisted agitation

Journal:	<i>Circuit World</i>
Manuscript ID	CW-03-2016-0006.R1
Manuscript Type:	Research Paper
Keywords:	printed circuit board, Megasonic agitation, copper, Electroplating, Acoustic streaming



1
2
3
4
5
6
7
8
9
10
11
12
13
14
15
16
17
18
19
20
21
22
23
24
25
26
27
28
29
30
31
32
33
34
35
36
37
38
39
40
41
42
43
44
45
46
47
48
49
50
51
52
53
54
55
56
57
58
59
60

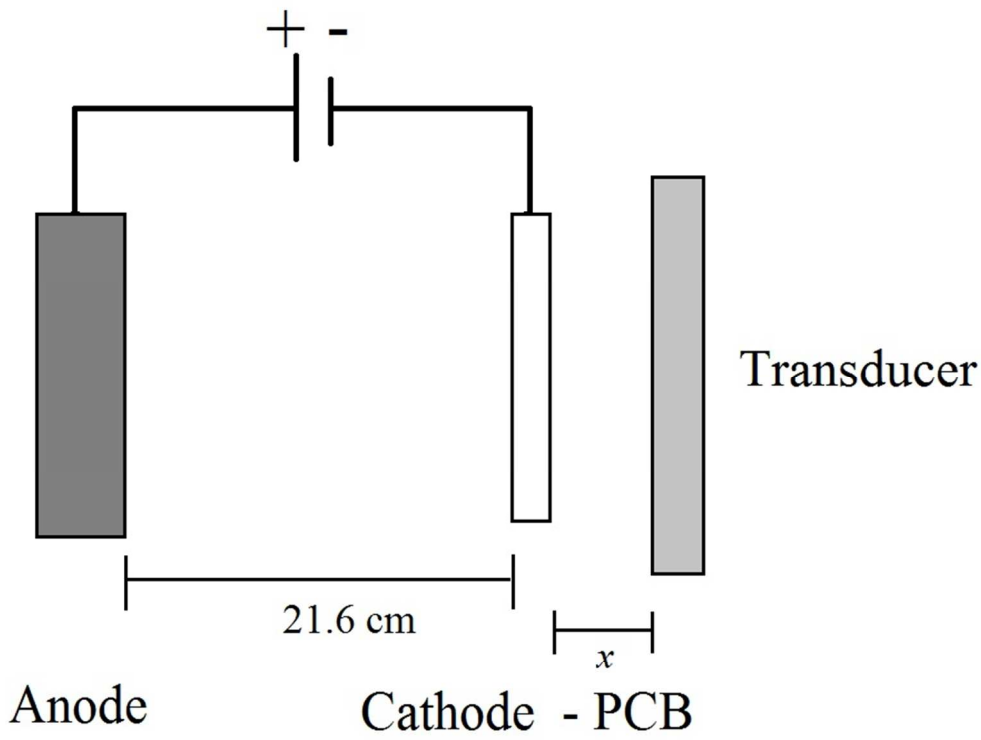


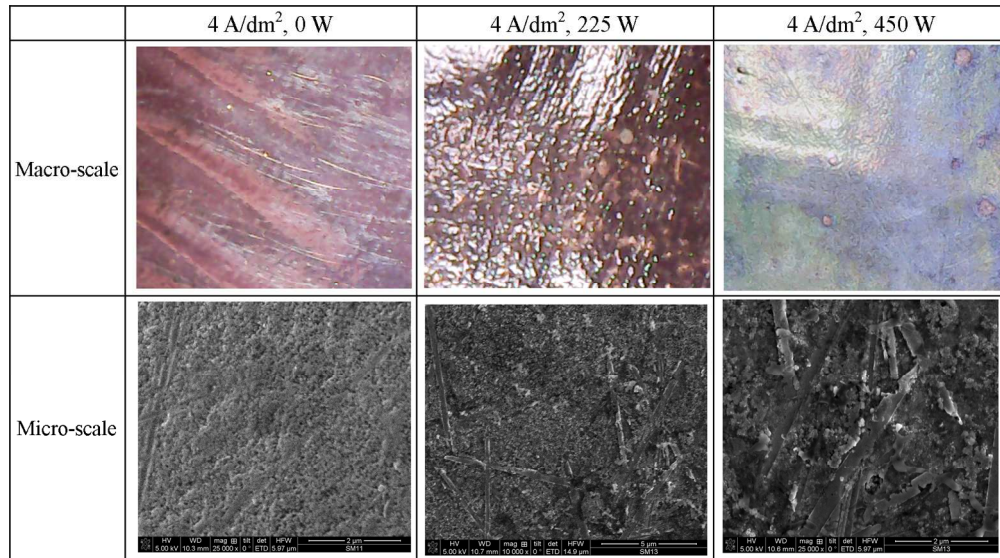
Figure 1 - A schematic of the plating cell setup indicating tangential distance x from PCB to transducer.

World

Experiment Number	Plating Parameter Altered	Experiment Plating Parameters		Measurement obtained	Purpose
		Transducer	Electrical Current Density (A/dm ²)		
1	Acoustic Power	Position : Tangential, $X = 1\text{ cm}$ Power : 0 W, 225 W, 450 W	4	Qualitative observations of Cu grain structure using an Optical and Scanning Electron Microscopes (SEM).	Reveals acoustic influence on surface chemical additives.
2		Position : Tangential, $X = 1\text{ cm}$ Power : 0 - 450 W	2	Quantitative measurements of Ra in response to changes in acoustic transducer power output, obtained using white light interferometer.	Notes how Ra changes with acoustic power output highlighting power-dependent influence on plated finish quality.
3		Position : Tangential, $X = 1\text{ cm}, 10\text{ cm}$ Power : 225 W	2	Quantitative measurements of Ra in response to changes to acoustic transducer tangential distance, obtained using a white light interferometer.	Notes how Ra changes with distance highlighting position-dependent influence on plated finish quality.
4	Electrical Current	Position : Tangential, $X = 1\text{ cm}$ Power : 225 W	1	Qualitative observations of Cu grain structure using SEM in response to current density variation across PCB surface.	Highlights distance dependent current thieving effect by transducer device and characterises adverse plating produced in response.
5		Position : Tangential, $X = 1\text{ cm}$ Power : 0 W, 225 W	2, 4	Qualitative observation of Cu grain structure using SEM in response to varying plating current densities.	Highlights changes to Cu crystallinity displaying acoustic influence on bath additives and potential performance issues.

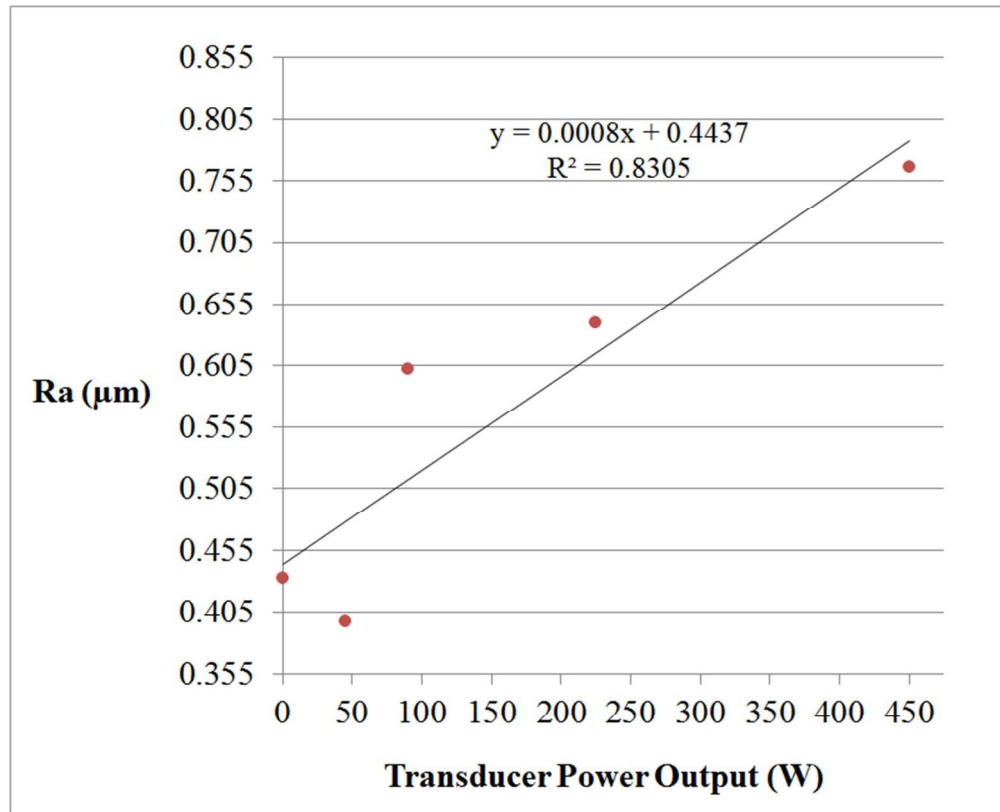
A list of the individual experiments with their parameters, measurement obtained and purpose.

1
2
3
4
5
6
7
8
9
10
11
12
13
14
15
16
17
18
19
20
21
22
23
24
25
26
27
28
29
30
31
32
33
34
35
36
37
38
39
40
41
42
43
44
45
46
47
48
49
50
51
52
53
54
55
56
57
58
59
60



Macro-scale and micro-scale SEM images for surfaces plated under silent (0 W) and MS-agitation (225 and 450 W).

Jiit World



A plot of Ra measured using a white light interferometer for an area 6.1 mm², highlighting the variation in response to transducer acoustic power output.

1
2
3
4
5
6
7
8
9
10
11
12
13
14
15
16
17
18
19
20
21
22
23
24
25
26
27
28
29
30
31
32
33
34
35
36
37
38
39
40
41
42
43
44
45
46
47
48
49
50
51
52
53
54
55
56
57
58
59
60

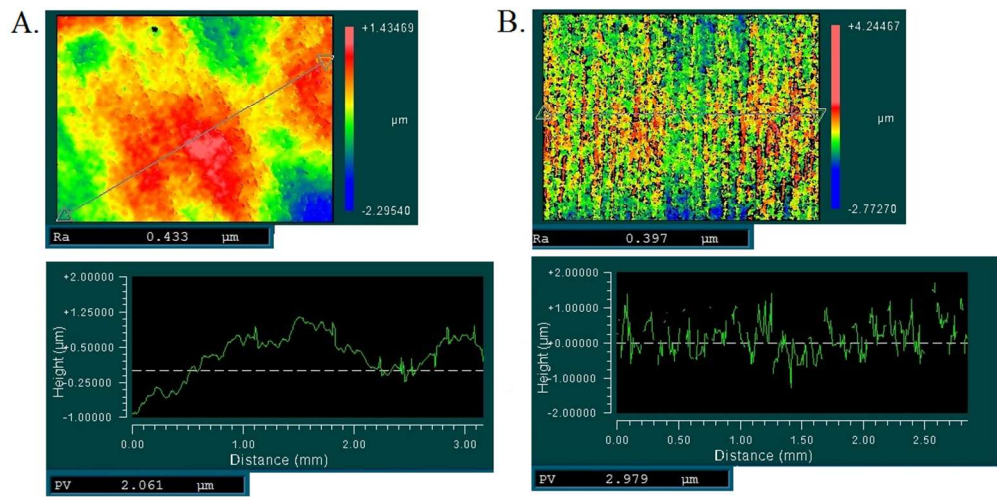


Figure 3 - Top-down images of PCB surfaces of areas 6.1 mm² using a white light interferometry with cross section profiles included underneath. Labels A and B indicate 0 and 45 W output power, respectively.

Circuit World

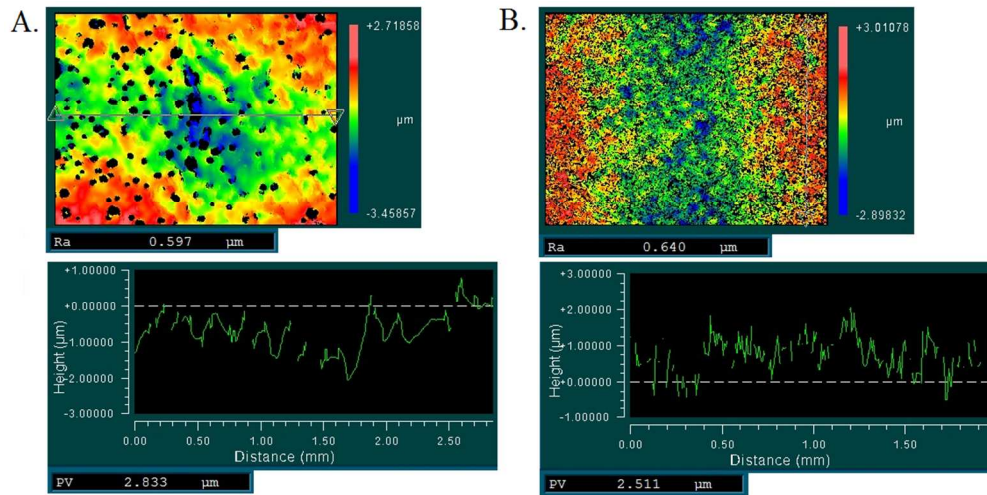


Figure 4 - White light interferometer plots of Cu plated PCB surfaces of areas 6.1 mm^2 , with cross-section profiles included underneath. A: transducer positioned 10 cm from the PCB. B: transducer is positioned at 1 cm.

Circuit World

1
2
3
4
5
6
7
8
9
10
11
12
13
14
15
16
17
18
19
20
21
22
23
24
25
26
27
28
29
30
31
32
33
34
35
36
37
38
39
40
41
42
43
44
45
46
47
48
49
50
51
52
53
54
55
56
57
58
59
60

1
2
3
4
5
6
7
8
9
10
11
12
13
14
15
16
17
18
19
20
21
22
23
24
25
26
27
28
29
30
31
32
33
34
35
36
37
38
39
40
41
42
43
44
45
46
47
48
49
50
51
52
53
54
55
56
57
58
59
60

	Low current density Frosting ($< 0.5 \text{ A/dm}^2$)	Standard plating behaviour for current density (1 A/dm^2)	High current density Burning ($> 2 \text{ A/dm}^2$)
Low Magnification			
High Magnification			

Table 3 - Plating behaviours observed during megasonic energy assisted electroplating.

Circuit World

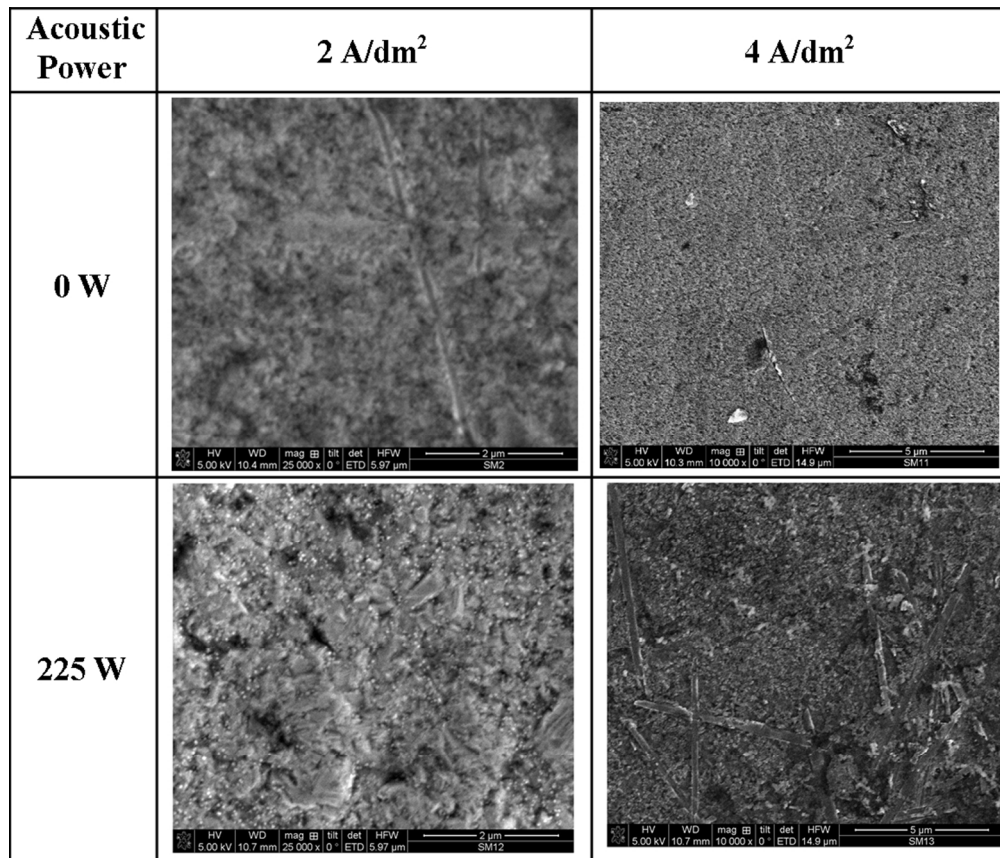


Table 4 - SEM images of PCB surfaces plated under varying current densities and MS-agitation.

1
2
3
4
5
6
7
8
9
10
11
12
13
14
15
16
17
18
19
20
21
22
23
24
25
26
27
28
29
30
31
32
33
34
35
36
37
38
39
40
41
42
43
44
45
46
47
48
49
50
51
52
53
54
55
56
57
58
59
60

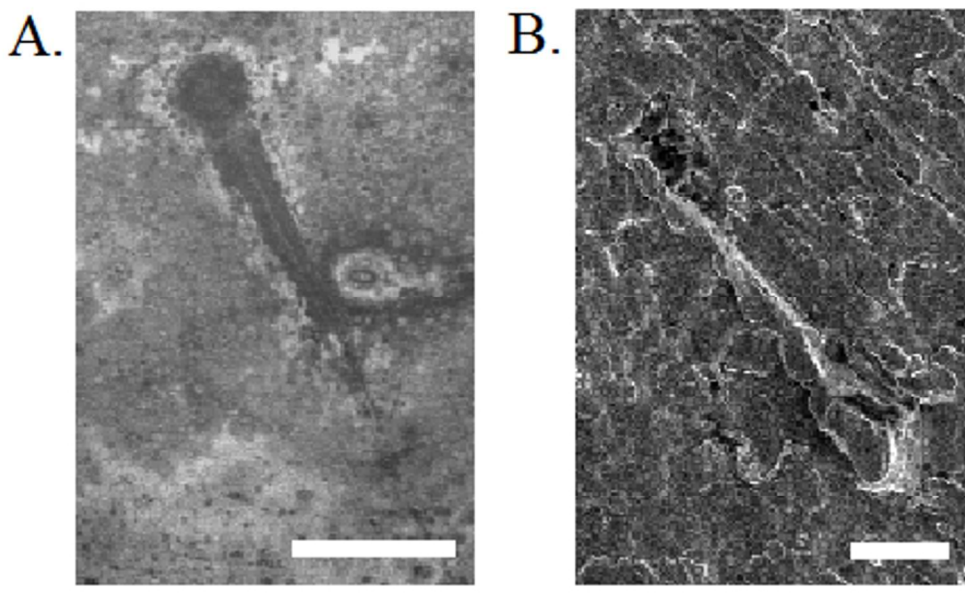


Figure 5 - Observations of megasonic assisted cavitation. A) Obtained using an interferometer, scale in image 1 mm B) SEM image, scale in image 5 μ m.

Circuit World

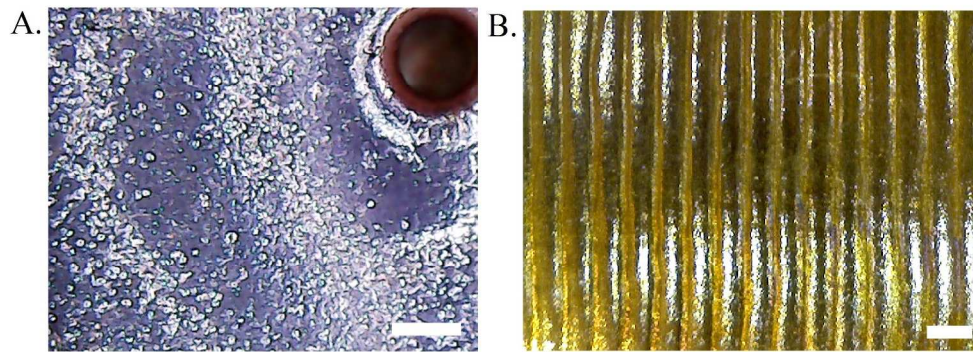


Figure 6 - Images of surface acoustic waves in electrodeposited copper. A) Formation of ringlets with scale bar 0.5 mm. B) Ridges with scale bar 1mm.

Circuit World

1
2
3
4
5
6
7
8
9
10
11
12
13
14
15
16
17
18
19
20
21
22
23
24
25
26
27
28
29
30
31
32
33
34
35
36
37
38
39
40
41
42
43
44
45
46
47
48
49
50
51
52
53
54
55
56
57
58
59
60

Morphology and acoustic artefacts of copper deposits electroplated using megasonic assisted agitation

Abstract

Purpose – A study of the influence of megasonic (MS) assisted agitation on Printed Circuit Boards (PCBs) electroplated using copper electrolyte solutions, to improve plating efficiencies through enhanced ion transportation.

Design/methodology/approach - The impact of MS assisted agitation on topographical properties of the electroplated surfaces studied, through a Design of Experiments (DOE), by measuring surface roughness, characterised by values of the parameter Ra as measured by white light phase shifting interferometry and high resolution scanning electron microscopy.

Findings – An increase of Ra from 400 nm to 760 nm measured after plating, for an increase to acoustic power from 45 W to 450 W. Roughening increase due to micro-bubble cavitation energy, supported through direct imaging of the cavitation. Current thieving effect by the MS transducer induced low-currents, leading to large Cu grain frosting reducing the board quality. Current thieving was negated in plating trials through specific placement of transducer. Wavy electroplated surfaces, due to surface acoustic waves, also observed reducing the uniformity of the deposit.

Research limitations/implications – The formation of unstable transient cavitation and variation of the topology of the copper surface are unwanted phenomena. Further plating studies using megasonic agitation are needed, along with fundamental simulations, to determine how the effects can be reduced or prevented.

Practical implications – Identify manufacturing settings required for high-quality MS assisted plating and promote areas for further investigation, leading to the development of an MS plating manufacturing technique.

Originality/value – Quantification of the topographical changes to a PCB surface in response to megasonic agitation and evidence for deposited copper artefacts due to acoustic effects.

Keywords Printed Circuit Boards, Megasonic agitation, Copper, Electroplating, Acoustic streaming

Paper type Technical paper

1. Introduction

Copper (Cu) electroplating is a technique employed for the metallisation of Printed Circuit Boards (PCBs) surfaces to allow individual layers to be electrically interconnected. ~~New methods of fine resolution electrodeposition are being sought which still offer economical manufacturing solutions, to support the~~

1
2
3 ~~increasing performance requirements within the PCB industry, such as larger aspect ratio, driven by a~~
4 ~~demand for a higher number of electronic components and stacking densities of PCB layer. The~~
5 ~~technological growth of high-value PCBs is currently driven by the development of boards which can~~
6 ~~propagate high frequency signals above 1 GHz (Okubo et al., 2013) with transmission speeds over 25 Gb/s~~
7 ~~(Muller et al., 2015) and at low bit error rates. Additionally, small track feature sizes are desired to allow for~~
8 ~~large board component densities. Successfully applying these properties introduces a strain on the~~
9 ~~manufacturability of the board, specifically related to a) the ability to fabricate small interconnects and b),~~
10 ~~the maintenance of a low signal error and on-board device component performance, despite increasing~~
11 ~~thermal transport issues due to higher power and denser board designs (Gurrum et al., 2012). These issues~~
12 ~~may be addressed in PCB construction through the fabrication of small diameter - less than 0.2 mm -~~
13 ~~Vertical Interconnect Access (VIA) interconnects of high thickness-to-width aspect ratio, which are~~
14 ~~uniformly filled with 100% Cu. Such interconnects would enable a) increased electrical and thermal~~
15 ~~conductivity, over the partially plated vias and b) multilayer fabrication with less thermally intensive~~
16 ~~bonding operations, increasing board lifetime and reducing fabrication costs. Such boards would be~~
17 ~~especially desirable in the mobile phone market which employs Cu filled THVs, of low aspect ratio of 4:1, as~~
18 ~~these currently require high fabrication costs due to special filling chemistry and plating waveforms (Roelfs~~
19 ~~et al., 2013).~~

20
21
22
23
24
25
26
27
28
29 A candidate method to enhancing the performance of traditional electroplating and providing Cu
30 filling is the introduction of a megasonic (1 MHz) transducer as a way to induce acoustic streaming to
31 enhance Cu ion transfer. The introduction of megasound has been shown to improve plating speed and filling
32 quality, on the electrodeposition of Cu in situations where the ratio between thickness down the via and on
33 the surface is close to 1:1 (Hyde and Compton, 2002, Costello et al., 2013).

34
35
36
37 Megasound (MS), defined here as sound waves of frequencies higher than 700 kHz, and ultrasound-
38 based (US) (0.02 MHz - 0.7 MHz) agitation processes generate different forces on the surface of a substrate,
39 which are induced either by acoustic cavitation or acoustic streaming flow. Cavitation is defined as the
40 formation of a bubble under sonication, produced as a result of localised fluid medium size variations, which
41 are brought on due to high tensile stresses occurring during the low pressure phase of an acoustic wave.
42 Depending on the life cycle and dynamics of the bubble, cavitation can be either stable or transient. Stable
43 cavitation describes the formation of bubbles, which, during their lifetime cycle, do not change significantly
44 in their equilibrium position or size. In contrast, transient cavitation, is the energy release through an
45 exothermic implosion, occurring from the collapse of air bubbles when local pressures in a fluid decrease to
46 below a minimum vapour pressure, defined as the absolute pressure, for a given temperature, at which the
47 liquid vaporises or is converted to a gas (Martin, 2013). The occurrence of cavitation depends on the
48 pressure, amplitude and frequency of an acoustic wave. At ultrasonic frequencies the transient cavitation
49 may cause considerable damage to a metal surface. The energy released depends on the size of the bubble
50 which is influenced by the frequency of the acoustic agitation. For MS frequencies the cavitation bubble size
51 is smaller than for US, as demonstrated in sono-luminescence studies which show that, at 1.056 MHz,
52
53
54
55
56
57
58
59
60

1
2
3 cavitation is produced from bubbles of diameters approximately 2 μm and 3 μm for ultrasound frequency of
4 0.647 MHz (Brotchie et al., 2009). Accordingly, agitation by US energy will create a rougher surface
5 topography, due to the more aggressive nature of the process, as demonstrated on a Cu surface (Verdan et al.,
6 2003). Similarly US energy is used in cleaning medical devices (Verhaagen and Fernández, 2016).
7
8

9
10 A sound wave traveling within a fluid medium induces a forcing effect per unit volume, governed by
11 the spatial variation of the Reynolds stress component of the acoustic wave. Such an effect generates a
12 steady streaming motion within the fluid along the propagation of the acoustic wave (Hoffelner et al., 2000).
13 At the interface of the bath solution/PCB a diffusion layer exists into which Cu cations are transported.
14 Increases in acoustic power and frequency enable thickness reduction of this layer due to acoustic streaming
15 convection (Abdollah et al., 2003). This reduction, in turn, increases the limited current density, which
16 enables a larger, more efficient plating reaction. For MS frequencies the layer is reduced further compared to
17 US, enabling access to higher limited current densities (Kaufmann et al., 2011).
18
19

20
21 Compared to US, MS offers less aggressive agitation due to the reduction in cavitation forces and
22 higher plating efficiency due to the reduction of the diffusion layer (Strusevich et al., 2013). Studies have
23 provided in-depth analysis of electrochemical behaviour during the plating trials; however, they have offered
24 a limited analysis of the changes in topography of the electrodeposits. A desired surface topography post-
25 electrodeposition, is a trade-off between the manufacturability of the PCB and its use for a given application.
26 A metal surface roughness of size 0.3 μm (Trelleborg, 2008) is efficient for manufacturing, as it enables
27 adhesion of dry-film resist and surface finish plating such as electrolytic silver. For high frequency (≥ 1
28 GHz) applications, a large surface roughness in the PCB manufacture would be undesirable, as electrical
29 signals transmitted through surface Cu features undergo increased bit error rates for surface roughness
30 increases (Okubo et al., 2013).
31
32

33
34 Understanding and controlling how deposited Cu roughness varies during processing is therefore
35 critical in introducing a successful surface modifying procedure into PCB manufacture. Research on US
36 agitation has included rigorous investigations to define its impact when used for metal surfaces (Verdan et
37 al., 2003, Cravotto et al., 2013). In contrast, little research has been carried out on the impact of MS-assisted
38 plating on Cu topography, excepting work highlighting that a polycrystalline finish was favoured (Kaufmann
39 et al., 2009). In response to this, the following article provides a Design of Experiments which studies the
40 impact of MS agitation on the PCB surface during standard Cu electroplating.
41
42

43
44 Changes to topography were quantified using the parameter R_a defined as the arithmetic average,
45 over a sampling length of area, of peak heights and troughs from the mean height of electrodeposits
46 (Peiponen et al., 2009). A visual characterisation of a surface after a plating cycle can be used to infer the
47 electroplating conditions under which the deposit was plated, as changes to plating settings alter Cu grain
48 size and thus the surface topography. The quality of a plated finish is characterised on the microscale by a
49 fine grain structure and on the macroscale by a shiny finish. A variety of plating finishes were obtained in the
50
51
52
53
54
55
56
57
58
59
60

MS trials performed. Through these trials, this article outlines some of the key effects observed on the plated Cu topography and highlights some of the unique plated artefacts produced in response to the MS agitation.

2. Experimental Investigation

The plating trials were performed on FR4 PCBs at Merlin Circuit Technology Ltd. based in Deeside, North Wales. The trials were performed in an experimental 500 L plating tank using soluble anodes. The plating schematic is indicated in Fig 1. The tangential distance of the anode basket to the cathode PCB is 21.6 cm. This setting has been optimised previously by Merlin Circuit for the plating bath geometry, as it maximises the plating uniformity across the PCB (Garich et al., 2007) and was applied in PCB manufacture prior to these investigations. The plating bath chemistry, intended for direct current (DC), pulse plating and periodic reverse-pulse plating (AC), was made-up using SLOTOCOUP CU110 supplied by Schloetter Ltd. When operating under the recommended electrolyte solution manufacturer's conditions, a high quality finish is produced, which is characterised as fine grained and ductile. The chemistry was comprised of 80 g/L copper sulphate, 100 ml/L sulphuric acid and 80 mg/L chloride. Chemical proprietary additives Cu 111 (5 mL/L) and Cu 114 (5 mL/L) were included in the solution.

The transducer system, manufactured by the Company Sonosys, is a square-faced submersible composed of four rectangular piezo-transducers, of size 2.5 cm by 11 cm, embedded in a steel sheet of 1.03 dm² area. The PZT outputs a 1 MHz \pm 0.05 MHz, acoustic wave with a variable power, where, at 100%, 500 W of electrical power is supplied to the piezoelectric emitter, which is converted to acoustic power output with a conversion efficiency of around 90%. The device was positioned tangentially to the PCB surface at a distance X within the plating bath using a scaffolding arrangement. The setup schematic is highlighted in Fig 1, with tangential distance altered according to the experimental setup. In all setups the acoustic wave within the bath was unidirectional due to the small beam spread angle attributed to high frequency acoustics (Brennan, 2007) and covered an area approximate to the area of the transducer face.

Figure 1 A schematic of the plating cell setup indicating tangential distance x from PCB to transducer.

2.1 Observation metrics and methods

After plating a sample was taken from the PCB of area 1 cm² using a Dremel 200 Multi-tool (RS), (UK). The sample was obtained from a region of interest for that investigation so as to highlight plating dynamics. The topography of the plating results was analysed using a Zygo Viewmeter white light phase shifting interferometer, at Heriot-Watt University, which measured the Ra over sample sizes scales 6.1 mm² and 24.4 mm² and provided 2D images of the PCB surface (zygo, 2016). The electrodeposited material was additionally evaluated from high-resolution images of the PCB surface, imaging between area scales 35 μ m² and 1.88 mm² using a Scanning Electron Microscope (SEM) also at Heriot-Watt University.

2.2 Design of Experiments

Experiments were grouped into those looking at changes induced by variations of the transducer acoustic power, and those occurring due to changes to the electrical current density. A series of five experiments were performed as displayed in Table 1, which highlights the individual settings applied, the measurement technique used to analyse and the purpose of the measurement.

A change in transducer output power alters the magnitude of the acoustic force on the surface of a PCB which in turn affects the Cu deposition. Categorising the impact of acoustic power on deposit properties provides a useful metric to control MS plating output. Experiments 1 – 3 altered the setup of the transducer, which, in turn, changed the acoustic power reaching the board surface. Experiment 1 used SEM and optical measurements of the surface to demonstrate how acoustic pressure influences the crystalline grain structure of the deposit; an important metric for defining quality. Experiment 2 investigated altered surface topography due to changes to the power output from the transducer from 45 to 450 W, for a fixed distance. Using the interferometer, measurements of Ra were taken and the values plotted on a graph for analysis. Plots of the changes in height over areas of 6.1 mm^2 were obtained and a qualitative analysis was made placing the observed features in the context of known plating behaviours and material compositions. Experiment 3 made changes to the transducer position to highlight variation in the electrodeposition. For example, increasing the distance of the transducer to the PCB alters the power of the acoustic wave when it reaches the surface due to attenuation (Etter, 1995). Measurements of Ra highlighted changes to surface topography in response to the transducer distance.

Changes of the Cu crystalline deposits were also investigated as a function of the electrical current. When fabricating a PCB the electrical current density is a key parameter for the control of the thickness and granularity of the electrodeposited metal. The layout of the electrical tracks on the surface of a board influences also the plating behaviour. For the plating dynamics to match quality and design specifications for the PCB customer, an operator needs to alter the electrical current settings to plate a desired thickness and morphology. To develop MS plating as a technique it is therefore important to characterise the behaviour of an electrodeposit in response to current variation, so as to highlight any adverse effects. Experiment 4 investigated the change to plated crystallinity across the PCB surface when the transducer was setup at a close distance, 1 cm, to the PCB surface. The transducer was setup with a close proximity to maximise the acoustic agitation reaching the PCB surface, at the expense of attracting current away from the PCB surface. Experiment 5 investigated changes to plating crystallinity in response to alterations to electrical current density. For both experiments observations were made from high resolution SEM images and height measurements, which enabled comparison to known topographies and structures for the conditions under which they were deposited.

Throughout the experiments adverse Cu artefacts were observed in the form of ripples and crater-like features on the surface of the PCBs after plating with MS agitation. These artefacts were analysed using qualitative observations of SEM and optical images, so as to identify the mechanism behind their formation and the processing parameters required to prevent them.

1
2
3 **Table 1** A list of the individual experiments with their parameters, measurement obtained and
4 purpose.
5
6
7

8 **3. Results and Analysis**

9 *3.1 Influence of Acoustic Power on Electrodeposit Properties*

10 *3.1.1 Experiment 1: Acoustic power impact on Cu grain structure*

11
12
13 A PCB Cu finish provides an indicator of plating quality, where a ductile and uniform coverage of
14 copper indicates a good plating process. If air pockets exist in a deposit then expansion of gas in the cavity
15 may cause the board to fracture and, in the worst case scenario, result in an opening of the electrical circuit.
16 Cu deposits can be categorised as either fine-grain, columnar or dendritic. A fine grain deposit is desired and
17 is characterised by high density, high uniformity and random crystal orientations. This deposit indicates the
18 correct operation of the plating bath parameters and is typically observed as a shiny plating finish. A
19 columnar structure includes deposits containing larger grains with an orientation perpendicular to the PCB
20 surface following grain boundaries. This deposit is not desirable as it induces a large variation in uniformity
21 on the PCB surface. A dendritic deposit, not observed during our trials, is a fibrous deposit of morphology
22 intermediate between the first two structures. Grain structure is influenced by all of the plating parameters,
23 where a change made to one parameter can induce an undesired grain structure change. For this reason, the
24 bath chemistry is carefully formulated by the chemical suppliers and maintained by the PCB fabricator, so as
25 to ensure a high quality electrodeposit (Yan et al., 2013).
26
27
28
29
30
31
32

33 The first experiment was plated under conditions highlighted in Table 2. The surface displayed a
34 shiny electrodeposit. From this observation, it would be predicted that the surface had a fine grain deposit
35 like the micro-scale image of the PCB plated under silent conditions as shown in Table 2. With MS [at 225 W](#)
36 [and 450 W](#), the micro-scale SEM images revealed however spiky, whisker-like randomly oriented grains. Cu
37 whiskers are characteristic of an electrodeposit formed by poor chemical additive performance and high
38 current density, and are different from dendritic deposits, which have a fractal-like appearance. The whiskers
39 were layered due to diffusion-limited aggregation of the Cu. The filament/granular nature of the Cu whisker
40 growth was possibly due to the uninterrupted crystal facets as they were quickly deposited on the PCB due to
41 the high current density. The random nature of the whisker orientation was likely due to the protruding tips,
42 which locally increased the electrical current density and enhanced their growth relative to the surrounding
43 uniform Cu structures (Minzari et al., 2011). The spiky deposits were not prevalent over the entire surface of
44 the PCB, enabling the appearance of a shiny deposit on the macroscale. Regardless, the spiky deposits
45 present are likely to cause issues for PCB quality, particularly with reference to its structural stability, as
46 large crystals are more susceptible to fracturing and breaking (Schlesinger and Paunovic, 2011). For this
47 reason the mechanical properties of the deposit may not be sufficient to match the Association Connecting
48 Electronics Industries (IPC) standards (Lee et al., 2010).
49
50
51
52
53
54
55
56
57
58
59
60

Table 2 Macro-scale and micro-scale SEM images for surfaces plated under silent (0 W) and MS-agitation (225 and 450 W).

3.1.2 Experiment 2: Interferometric measurements of R_a of PCB surface as a function of transducer power variation

The second experiment was performed to investigate the influence of the transducer power output on the plated surface finish. Measurements of R_a was obtained using a white light phase shifting interferometer and plotted against power increase, as displayed in Fig 2. For each measurement, the transducer was set up and the plating settings chosen as indicated in Table 1. R_a increased by 205% as the output power increased from 45 to 450 W. Between 0 W and 45 W there was a 9% decrease in R_a .

It is possible that the natural variation of roughness due to the glass weave influenced the result, adding a random variation to the data. A PCB is comprised of a glass weave encapsulated in an epoxy resin. The weave causes a natural large scale height variation, defined as waviness, of around 6 μm across the PCB surface (IPC, 1999). When evaluating R_a the sample length is chosen so that the long wavelength features do not interfere with the calculation. The sampling length area chosen should be large enough to encompass the small-wavelength (roughness) features, yet small enough so that it does not include the large-wavelength (wavy) features. If the sampling length is increased to include the wavy features then the R_a parameter will be influenced by this and increase. To highlight this further, data from the interferometer was used to plot top-down images of the electroplated surface for 0 W and 45 W as indicated in Fig 3. Under silent conditions the wavy features were observed on the PCB contributing to an approximate 2 μm Peak-to-Valley height. When 45 W MS agitation was applied, the surface displayed considerable micro-roughening, which was not detected by the interferometer in the evaluation for R_a , highlighting measurement device limitation. The reduction in R_a measured from 0 W to 45 W could be accounted for by the wavy features on the PCB and as such, the roughness increase at 45 W highlighted in the cross-section profiles in Fig 3, was not measurable using the interferometer. To detect the influence of the transducer at low acoustic outputs, for this reading a smaller sampling area would have had a greater chance of measuring the roughness variation, although this would have been closer towards the detection limit of the device should have been used.

For transducer powers larger than 45 W an increase in roughness was measured for an increase in pressure output. At 90 W the roughness was significantly large so that the wavy features on the board did not interfere with the measurement. A linear dependence of R_a was indicated on the plot. The increases in roughness measured with increasing transducer powers are most likely due to cavitation effects, where higher acoustic pressures enhanced the frequency of the cavitation effects (Ebnesajjad, 2010), as observed when the transducer was setup at smaller distance scales. The cavitation damage influencing R_a is more difficult to quantify as a function of acoustic pressure as it depends on localised variations in fluid medium density, bubble diameter size, and bath chemical composition and temperature (Brotchie et al., 2009). An

analysis into these individual effects and their impact on R_a is required, to derive a relationship and make predictions on the behaviour of the acoustics on R_a . This analysis is beyond the scope of this article.

It is uncertain over which area-scale the impact on roughness, due to cavitation forces, was most evident, although they are observable over the 6.1 mm^2 scale. At this scale, the results show that the natural undulations of the PCB laminate impact on the measurement for surface roughness, making it difficult to extract their influence at low power outputs but was possible at 90 W and higher.

Figure 2 A plot of R_a measured using a white light interferometer for an area 6.1 mm^2 , highlighting the variation in response to transducer acoustic power output.

Figure 3 Top-down images of PCB surfaces of areas 6.1 mm^2 using a white light interferometry with cross section profiles included underneath. Labels A and B indicate 0 and 45 W output power, respectively.

3.1.3 Experiment 3: Interferometric measurements of R_a as a function of distance between transducer and PCB

The aim of the third experiment was to highlight how an increase of the distance between the transducer and the PCB alters the surface roughness of the electrodeposit formed, as the acoustic streaming force is reduced on the surface. Highlighted in Fig 4 are two top-down images of the 6.1 mm^2 PCB surface area. Variations in height are indicated by changes of colour and by the cross section profiles. The labels A and B highlight two different PCBs plated with the transducer setup at distances of 10 cm and 1 cm, respectively, under conditions outlined in Table 1. Dark regions in the figure can either be due to steep and vertical protrusions, depressions, or saturation of the detector due to high reflectivity of the surface. In A, these dark pixels are large in size whereas in B, they are more numerous but smaller in size. These features are observed only on PCBs which have undergone MS agitation. It is uncertain from the image if the features are peaks or depressions, although it is likely that they originate from cavitation features, as discussed in the introduction. If this is the case, then the reduction of pressure of the acoustic wave due to the increase in transducer distance encourages the formation of larger cavitation features (Hauptmann et al., 2013). The qualitative results highlight that closer transducer distances increase the micro-roughness of the PCB surfaces, where smaller cavitation-sized features are favoured. The profile height variations for A and B reveal a maximum Peak-to-Valley variation of $2.83 \text{ }\mu\text{m}$ and $2.51 \text{ }\mu\text{m}$, respectively, which are comparatively similar.

When comparing to silent conditions highlighted in Fig 3A, the roughness R_a increased by 37% and 47% for the transducer positioned at 10 cm and 1 cm accordingly. This shows that with MS agitation the

1
2
3 surface roughness increased significantly at large acoustic powers (225 W) as observed in section 3.1.2. As
4 the transducer is positioned from 1 to 10 cm away from the PCB surface, measurements of Ra reveal an
5 increase in surface roughness of 7%. This variation is relatively small and could be accounted for by random
6 errors in the data, brought on by the large wavy features across the PCB surface, as explained in section
7 3.1.2. When sampling the PCB surface it was difficult to choose a sample area to accommodate for the
8 waviness of the PCB as the cavitation features varied in size. A sampling length smaller than 6.1 mm^2 would
9 miss the features highlighted in Fig 4A, but not the features in Fig 4B (ASME, 2010).

10
11
12
13
14 Using the interferometer, measurements of Ra and Peak-to-Valley distances indicated little
15 quantifiable variation between the two surfaces, although plots of the two surfaces displayed qualitative
16 differences in micro-roughening. This highlights that, as the transducer-PCB distance is reduced with
17 corresponding increase of transducer power, the larger resulting pressure increases the frequency of the
18 cavitation but not its magnitude as indicated by Ra .

19
20
21
22
23 **Figure 4** White light interferometer plots of Cu plated PCB surfaces of areas 6.1 mm^2 , with cross-
24 section profiles included underneath. A: transducer positioned 10 cm from the PCB. B: transducer
25 is positioned at 1 cm.
26
27
28
29

30 31 3.2 MS plating variation in response to electrical current density

32 3.2.1 Experiment 4: Influence of transducer position on the electrical current distribution

33
34 The fourth experiment explored how changes to transducer position altered the deposited Cu
35 crystalline properties, through changes of the electrical current distribution. The transducer was positioned 1
36 cm away from the PCB surface and toward the centre. The PCB size was 5.20 dm^2 which was larger than the
37 1.03 dm^2 area undergoing agitation. The PCB was plated at 225 W acoustic power output with an electrical
38 current density of 1 A/dm^2 . After the plating cycle, three Cu finishes were witnessed across the surface and
39 characterised by (1) a sandpaper-like texture appearing as shiny frost-like speckles at the centre of the PCB,
40 (2), a smooth bright finish surrounding the middle frosted region and (3) a nodular, powdery dark finish at
41 the edge of the PCB. SEM images of the individual surfaces are displayed in Table 3 at high and low
42 microscope resolutions. As explained later, the three finishes are characteristic of changes brought on by
43 variations to the electrical current distribution and the behaviour of the chemical additives across the PCB.
44 Such changes have been reported elsewhere (Dini, 1993), predicting how the crystalline behaviour changes
45 in appearance and texture from observations on the macro-scale and micro-sale. For electroplating under
46 current settings lower than 0.5 A/dm^2 , the SEM images show that large Cu face-centre-cubic crystals
47 assemble themselves in a cubic arrangement of larger crystals. The deposit is columnar in nature, which
48 suggests that the deposition occurs along individual grain boundaries (Kocks et al., 2000, Wang and Y.
49 Huang, 2014). Evidence for individual monolayers was highlighted on the cubic structure in the high-
50
51
52
53
54
55
56
57
58
59
60

1
2
3 resolution image. These layers were formed from the Cu cations being deposited from the solution onto the
4 crystal face, indicating a step layer growth mechanism. Gaps exist between the larger crystal structures
5 which give the deposit a highly brittle structure. During thermal cycling, such copper would undergo
6 fracturing, due to the expansion of the air pockets resulting in the degradation of the PCB. If the electrical
7 current levels are set up correctly and the bath chemistry is properly maintained, then a frosted finish will not
8 be observed after plating. The appearance of the frosted finish here is due to the presence of the metallic
9 transducer, reducing the plating current across the PCB. The electrically conductive surface of the transducer
10 acts as a current thief reducing thereby the effective current density at the PCB surface. This effect has been
11 reported in other sono-electrochemical experiments (Coleman and Roy, 2014). At the regions where current
12 was stolen, the surface of the metal deposited on the PCBs shows a frosted finish indicative of plating at
13 extremely low current densities. Further studies not reported here show that, on increase of the distance
14 between the transducer and the ~~PCB-transducer~~, the current thieving effect reduces to zero. This was
15 measured by the appearance of the Cu finish and the plated thickness. It was found that current thieving is
16 negligible when the transducer is placed tangentially at 4.5 cm from the PCB surface. The frosted finish
17 covered an area smaller than the area of the acoustic agitated area. Around the periphery of the frosting a
18 bright and shiny Cu finish was deposited. SEM images obtained within this region, as shown in Table 3,
19 highlight a compact fine grain growth of Cu, which is indicative of the standard plating behaviour expected
20 for correct operation of the current settings and appropriate additive concentration levels. A PCB fabricated
21 with this finish will not undergo thermal cycling issues and is desirable as a final product.
22
23
24
25
26
27
28
29
30
31
32

33 **Table 3** Plating behaviours observed during megasonic energy assisted electroplating.
34
35
36
37

38 At the edge of the PCB a burnt finish was observed. Burning is a standard plating error highlighted
39 by a nodular, dark-brown, powdery deposit formed in regions where the current density exceeds the limited
40 current density, which is typically at the edge of a PCB or on isolated Cu tracks on the board surface
41 (Schlesinger and Paunovic, 2011). The limited current density influences the operational limit of the current
42 supplied to the PCB. Beyond this value the Cu cation depletion rate at the surface of the PCB is higher than
43 the repletion rate so as long as the fluid convection is constant. An SEM image of a burnt finish is provided
44 in Table 3 at low (20 μm on scale) and high (500 μm on scale) magnifications. The finish is characterised by
45 micro-nodules of Cu which vary in size from 5 to 250 μm in diameter. The variation in nodule size is
46 possibly due to the fast build-up of Cu on the smaller nodules which act as nucleation sites for the larger
47 ones. A burnt finish is characterised by a weak deposition and is undesirable in PCB fabrication.
48
49
50
51
52

53 When plating under MS assistance, previous work performed indicated that the inclusion of standard
54 bath agitation techniques such as panel movement and/or air bubbles caused disruption and negated some of
55 the benefits of acoustic wave agitation. For this reason, when plating under MS conditions, these two
56 techniques were not included. The inclusion of panel movement and bubble agitation enables replenishment
57
58
59
60

of depleted cations near the PCB surface. With the introduction of MS agitation the acoustic streaming currents produced near to the PCB surface provide the same role, enabling higher currents to be applied before burning occurs. Under the plating setup the PCB size was larger than the area agitation by the MS and so, at the edges of the PCB, the MS acoustic streaming failed to spread, reducing the streaming force and the limited current there, thus inducing burning for the current supplied. Further studies have shown that, to prevent burning during MS plating, changes to the transducer position can be made which increase fluid circulation across the PCB. Increasing the tangential distance increases the spread of the acoustic wave across the PCB up to a point, at the expense of reduced acoustic power due to attenuation of the travelling wave. To prevent burning and frosting from occurring entirely on a board, multiple transducers could be deployed, directed at different regions on the PCB, or a transducer the size of the desired area to be plated could be implemented. Under these settings a plating finish would be obtained as highlighted in Table 3 under the standard plating column, where small variations in particle size and fine grain deposition are obtained.

3.2.2 Experiment 5: Cu crystallinity variation with current density

A key parameter controlling the growth of Cu is the electrical current density. If the bath chemistry is maintained within a set range, then the growth of the Cu is proportional to the current density applied (Sivasankar, 2008). SEM images of the PCB surface plated under different current density regimes are provided in Table 4. Under silent conditions the Cu was plated at 2 A/dm² and 4 A/dm². These surfaces displayed no discernible differences and were characterised by a uniform fine grain deposition. When MS plating at 225 W and with the same current densities, the SEM images revealed different plating finishes to those produced under silent conditions. For MS plating at 2 A/dm², a uniform surface deposition was observed, although a large polycrystalline deposit was also apparent. For MS plating at 4 A/dm², a spiky whisker-like growth was observed, as discussed in section 3.1.1. The cause behind the polycrystalline and the whisker formations suggested that the bath additives were performing incorrectly. The plating bath additives Cu111 and Cu114 enable grain refinement of the Cu deposit and a failure of their behaviour can lead to large grain deposits.

Table 4 SEM images of PCB surfaces plated under varying current densities and MS-agitation.

The poor performance of the bath additives could be explained by their low concentrations near the PCB surface due either to the force of acoustic streaming waves on the PCB surface, which can remove organic molecules, similar in structure to the bath additives, off a surface (Hennig et al., 2009), or by denaturing the additives under large thermal increases, brought on by megasound cavitation (Hauptmann et al., 2013). In additional plating trials, reductions in acoustic pressure have shown to improve the condition of

1
2
3 the surface finish up to a point, after which, the reduction in electrolyte transport produces an undesirable
4 burnt finish, as explained in section 3.2.1.
5
6

7 8 **4. Copper artefacts due to MS plating**

9
10 Acoustic assisted plating has been shown to strongly influence the characteristics of electrodeposited
11 Cu. A variety of other plating effects have also been observed in experiments 1-5, which are attributed to
12 acoustic artefacts from the MS interaction with the electrodeposit. The artefacts include cavitation and
13 periodic copper features. These plating effects are discussed along with their potential impact on PCB
14 fabrication.
15
16

17 18 *4.1 Megasonic induced cavitation features*

19
20 Cavitation is a unique artefact observed under acoustic agitation. It varies in intensity and magnitude
21 depending on the acoustic pressure and frequency. Cavitation has been widely reported under US agitation
22 (Gale and Busnaina, 1999). Cavitation can be observed on a surface because of the damage caused when
23 highly pressurised thermal energy is released from bubble collapse. The damage is typically observed as
24 crater-like features, although it may also be manifested as a micro-roughening of the surface. The energy
25 released is observed as a jetting micro-stream. The jet stream is typically directed tangentially towards the
26 surface the bubble is against, although it is possible for the jet stream to become directed along the surface, if
27 the bubble undergoes influence from external, directional convection currents (Zhou and Gao, 2013).
28
29

30
31
32 Fig 5A presents an example of cavitation observed during one of the investigations on a PCB surface
33 plated under MS. The circle, of diameter of around 400 μm , is possibly a crater nucleus from where the
34 bubble imploded and the tail of length of about 2 mm is the jet stream, as the bubble was directed along the
35 surface by acoustic streaming currents. These features are characteristic of acoustic cavitation and are not
36 observed under standard plating. A high resolution SEM image of a MS plated PCB surface is given in fig
37 5B. Features are present which appear similar to the cavitation measured on the larger scale. The features,
38 many of them occurring on the surface with the same orientation, appear to display the same nucleus and tail
39 features, albeit at a smaller scale. Previous studies into cavitation influences have indicated that some
40 cavitation, occurring at high frequencies (1 MHz), would be on a scale too small to be detected by standard
41 employed techniques such as sono-luminescence (Gale and Busnaina, 1999, Lucke and Beecham, 2009). The
42 cavitation features are, to the best of the authors' knowledge, the first examples ever recorded for plated
43 copper surfaces.
44
45

46
47 Circle features and pits were readily observable on the PCB's surface after MS plating. They varied
48 in size and could be observed by eye on the macroscale down to the microscale. The increase of roughness
49 mentioned in sections 3.1.2 and 3.1.3, could have been brought on by micro-cavitation features.
50
51
52
53
54
55
56
57
58
59
60

1
2
3 **Figure 5** Observations of megasonic assisted cavitation. A) Obtained using an interferometer,
4 scale in image 1 mm B) SEM image, scale in image 5 μm .
5
6
7

8 9 *4.2 Measurements of copper ridges and surface acoustic waves*

10 When an MS wave is directed onto a PCB surface, a part of the wave may be scattered and then
11 confined to a thin layer near the board surface. The conditions for this confinement depend on the free
12 acoustic wavelength, the acoustic impedance at the board surface and the angle scattered. The confined
13 evanescent waves are called Rayleigh-wave Surface Acoustic Waves (SAWs), which exponentially decay
14 perpendicularly to the board surface (Rienstra and Hirschberg, 2013). SAWs travel in the plane of the board
15 and are an example of boundary layer acoustic streaming. If a SAW is generated on a rigid surface which has
16 had organic molecules attached, it is seen that the molecules are being displaced. If the additives in a plating
17 bath behave in the same manner, they may become displaced into nodal regions which exist between the
18 oscillating high and low pressure maximums within the SAW (Hennig et al., 2009). Additive movements
19 may occur in a periodic fashion where regions of high and low density are formed, separated by half of the
20 acoustic wavelength, λ .
21
22
23
24
25
26

27 Under MS plating Cu features separated by $\lambda/2$ have been observed, as shown in Fig 6. Fig 6A
28 shows a top-down image of concentric ringlets emanating from a tooling hole on a PCB. The ringlets
29 appeared as periodic deposits of large-grain Cu growths which were observed as a dull finish on the PCB.
30 The distance between the ringlets was around 0.7 mm, which corresponds to $\lambda/2$ of the 1MHz wave in the
31 electrolyte solution. The appearance of the periodic ringlets suggest the generation of a SAW on the PCB
32 surface. The ringlets are characterised by a deposition of large grains and a possible mechanism for their
33 formation is that they are due to low concentrations of additives at the SAW pressure maxima. In turn, in the
34 pressure nodal regions, the additives would congregate, increasing in concentration and encouraging a shiny,
35 fine grain deposit in between the matt-finished ringlets.
36
37
38
39
40

41 The SAW influence on plating is not limited to changes in plating finish. Variations to Cu thickness
42 were also observed on the PCB surface, as shown in Fig 6B where periodic ridges are observed on an MS
43 plated PCB surface. The ridges are separated again by around 0.7 mm and are characterised by peaks and
44 valleys. Ridges occurred on both sides of the board, although, during some trials, they would appear greater
45 on one side of a panel rather than the other. This was possibly due to the interplay between the absorption
46 and transmission of the wave through the PCB. The ridge orientation was typically vertical to the board
47 orientation in the bath and changes to the angle of incidence of the acoustic waves altered their positions and
48 orientation across the surface. Motions in either the panel or the transducer appeared to alter the position of
49 the ridges. If cathode rail movement was included, the occurrence of the ridges on the board would be
50 reduced, although it would not entirely subside. The MS plated Cu finish on the ridges appeared shiny,
51 which suggests the correct behaviour of the brightener additives and the formation of a fine-grain deposit.
52 The possible reason as to why a dull finish was not observed could be related to the formation of stable
53
54
55
56
57
58
59
60

1
2
3 cavitation. Unstable cavitation would lead to a dull matt finish due to improper additive behaviour, as
4 explained in section 3.2.2. Despite the desired shiny uniformity of the Cu finish, the ridges induced a
5 variation of 20 μm in plating uniformity as measured from cross-sections. This variation is larger than the
6 minimum acceptable by IPC specifications and so the ridges in their current form are an undesirable artefact.
7
8
9

10
11 **Figure 6** Images of surface acoustic waves in electrodeposited copper. A) Formation of ringlets
12 with scale bar 0.5 mm. B) Ridges with scale bar 1mm.
13
14

15 16 17 **5. Conclusions**

18 *5.1 Whisker growth due to high electrical currents and MS power*

19
20 MS plating trials investigated the influence of the acoustic power emitted by the transducer on the
21 characteristics of the electrodeposits. On maximum acoustic output power, 450 W, observations on the
22 macroscale revealed a shiny electrodeposit on the surface, which was expected for standard fabrication and
23 suggested a fine-grain ductile microscale finish. On observations of its microstructure the Cu structure
24 appeared spiky, with large whisker-like formations. Whisker growths were also observed during MS plating
25 with high electrical currents of 4 A/dm^2 . Whisker growth is undesirable and was the product of the high
26 electrical currents and the large acoustic powers. The acoustic power induces an acoustic streaming force on
27 the PCB surface as well as exothermic MS cavitation. The two effects combined could have a negative
28 impact on the organic chemical additives on the PCB surface, which under typical plating operation, ensure
29 grain refinement.
30
31
32
33
34

35 Thermal increases brought on by MS cavitation effects could induce denaturing of the additives and
36 the acoustic streaming force could displace and remove the attached organic molecules. A whisker-like
37 deposition is undesirable in PCB fabrication due to its susceptibility to fracturing and breaking under thermal
38 expansion, leading to reduced PCB life time and electrical shorts. To reduce the impact of this plating finish,
39 modifications to the MS plating cycle could be implemented, such as the introduction of an off-cycle during
40 the plating cycle, or plating on lower current densities and acoustic powers.
41
42
43
44
45

46 *5.2 Micro-roughening due to transducer position alteration and power change*

47 The introduction of MS agitation increased micro-roughening on the plated PCB surface. The micro-
48 roughening appeared to increase with increases in transducer power output and on the reduction in distance
49 of the transducer device. For smaller tangential transducer/PCB distances, attenuation of the acoustic wave
50 was less, enabling higher acoustic powers over the PCB surface per unit area. An increase in acoustic power
51 is realised by increases in pressure. Increases to acoustic pressure are reported to increase the intensity of
52 cavitation collapse (Ebnesajjad, 2010) and so, the micro-roughening behaviours witnessed could be
53 accounted for by an increase of cavitation power on transducer distance reduction and power output increase.
54
55
56
57
58
59
60

1
2
3 Controlling roughness on a plated Cu surface is important as roughness impacts on PCB
4 manufacture, where increases in manufacturing performance are obtained for increases to roughness up to a
5 point where further increases led to electrical signal loss at high operating electrical frequencies.
6
7

8 The current trend in PCB design is towards high interconnect density, high-frequency applications
9 (Beers and Minten, 2011). The introduction of MS plating aims to reduce interconnect features on a PCB,
10 reducing track pitch and providing low surface roughness of metal tracks for high frequency applications.
11 The surface roughness values measured as a result of the MS are larger than desired for high-frequency PCB
12 fabrication. Fabricating under these conditions is currently counterproductive for the development of future
13 product technological trends. A reduction in roughness during MS plating could be made by making
14 modifications to the plating cycle. Reducing the acoustic pressure output towards the end of a plating cycle
15 would ensure that the plating finish at the end of the cycle would undergo less cavitation and a more uniform
16 finish. Additionally, introducing an off-cycle during plating would on average reduce the cavitation
17 influence. Further studies are required into the influence of more complex MS plating cycles where on/off
18 duty cycle and acoustic pressure are altered.
19
20
21
22
23
24
25

26 *5.3 Current distribution due to current thieving.*

27 Observations were made as to how the electrical current distributed across the PCB due to a current
28 thieving effect, along with the acoustic streaming force reduction, influences the crystallinity of the
29 electrodeposited metal. A spectrum of plating behaviours was observed which are characteristic of high and
30 low plating currents. The behaviours were induced primarily due to a transducer-distance related effect,
31 brought on by the thieving of electrical current away from the PCB. The current variation induced by the
32 close proximity of the device to the cathode surface, produced the low quality plating finish. To enable a
33 high quality finish whilst applying the MS, it was found that increasing the transducer tangential distance
34 reduced the current thieving effect. At around 4.5 cm from the PCB the finish variation was negligible and a
35 bright and shiny finish was produced. The results show that, to form a high-quality bright plating finish when
36 MS plating, a minimum tangential distance must be found for the transducer device being used. This value
37 may alter depending on the size and shape of the transducer. Further electrochemical investigations are
38 required to assess more thoroughly the influence of transducer surface conductivity on current thieving, as
39 changes may be made to the transducer surface to reduce electrical conductivity, such as the deposition of a
40 non-electrically conductive layer.
41
42
43
44
45
46
47
48

49 When the acoustic streaming force failed to cover the entire face of the PCB, the Cu cation
50 replenishment rate suffers in electrically isolated regions, inducing unwanted burning of the Cu deposit. This
51 result shows that, for the effective fabrication of a PCB when MS plating, the acoustic agitation must cover
52 the total plated area, especially if the panel movement and bubble agitations are switched off.
53
54
55
56
57
58
59
60

5.4 MS Acoustic plating artefacts

Unique MS acoustic agitation artefacts were observed on the electrodeposited Cu. These were possibly generated by the formation of SAWs on the PCB surface in response to back reflections of the acoustic wave. In PCB manufacture the presence of a SAW is detrimental to Cu uniformity. To enable a uniform deposition of Cu, the formation of a SAW should be prevented by reducing the occurrence for resonant acoustic frequencies to form on the PCB. One method is to vary the frequency output from the transducer, by either sweeping across a finite range (Erpelding et al., 2007) or randomly switching between values (Tang and Clement, 2009b). Frequency variation suffers from issues of low power coupling into individual acoustic modes, which may or may not be critical in MS plating. An alternative method is to alter the phase of the acoustic wave over discrete time intervals, known as phase-shift-keying (PSK)(Tang and Clement, 2009a). PSK has been demonstrated at ultrasound frequencies and produces improved standing wave reduction performance, but without any drastic change to the frequency output. When installing a transducer for use in MS plating, frequency shifting and or phase shifting should be considered, although the addition of these features increases the costs of the device.

5.5 Sub-micron bubble influence on plating

MS has been introduced into PCB plating to investigate improved Cu deposition in terms of uniformity within fine feature THV interconnects. Increasing fluid transport is a critical factor for the increase of plating uniformity down THVs due to the enhancement of electrolyte transport. It is difficult to induce fluid convection down THVs of high aspect ratio (10:1) and small diameter size (< 0.3 mm) due to the increased influence of viscous forces over inertial forces. Previous simulations have highlighted that the increases to forced streaming currents by MS acoustics are weak, so as to not significantly contribute to fluid transport down high aspect ratio vias (Strusevich et al., 2013). Regardless, increases to plating efficiencies have been observed (Costello et al., 2013).

Evidence for sub-micron bubbles was witnessed on the MS plated PCB surfaces from images of micro-cavitation. Under megasonic agitation, acoustic streaming is produced, causing microbubbles in solution to be transported within the streaming current. A secondary influence on fluid transport is the potential increased movement of solution due to the passage of these microbubbles (Cravotto et al., 2013). This effect has been reported under ultrasound agitation and evidence of enhanced fluid convection around the microbubbles has been provided in terms of Particle Image Velocimetry measurements and simulations using the COMSOLTM software package (Collis et al., 2009). The presence of sub-micron bubbles observed on the PCB surface during the investigations, suggests that they could influence the plating deposition properties, as do microbubbles in US plating and could be an influential factor in improving fluid transport in and around the THVs, enabling the plating enhancements witnessed. Few simulations have been made into the potential for increased electrolyte transport due to sub-micron bubble transport. New and improved models behind the plating interactions are required to develop the mechanism for MS fluid transport, which

in turn can be used to successfully manipulate and control the positive plating benefits, and overcome the issues brought on due to unstable cavitation.

5.6 Overall conclusion

MS introduction into electrochemistry is a relatively new field of study and its potential positive impact on fabrication is contended by adverse plating effects. Despite the initial shortcomings of the technology, remedies exist, although each requires a re-evaluation of the plating bath parameters. To bring about the ever-demanding increases to PCB technological development, alterations to the electrochemical setups may be required which mirror this changing landscape. Megasound technology could play a key role in this future, however further electrochemical and sonochemical investigations are needed before implementation can take place in a PCB fabrication line.

Bibliography

- Abdollah, S., Banks, C. E. & Compton, R.G. (2003). "Ultrasonic effects on the electro-reduction of oxygen at a glassy carbon anthraquinone-modified electrode. The Koutecky–Levich equation applied to insonated electro-catalytic reactions". *Physical Chemistry Chemical Physics*, **5**, pp. 3988 - 3993.
- Asme (2010). *Surface Texture: Surface Roughness, Waviness and Lay*, American Society of Mechanical Engineers.
- Beers, J. & Minten, K. (2011). "PCB technology Future Trend". *IEEE 802 LAN/MAN Standards Committee*. Available at: http://www.ieee802.org/3/bj/public/nov11/minten_01a_1111.pdf (Accessed 1 March 2016).
- Brennan, R.E. (2007). *Ultrasonic Nondestructive Evaluation of Armor Ceramics*, Rutgers The State University of New Jersey - New Brunswick.
- Brotchie, A., Grieser, F. & Ashokkumar, M. (2009). "Effect of Power and Frequency on Bubble-Size Distributions in Acoustic Cavitation". *Journal of Physical Review Letters*, **102**, pp. 1- 4.
- Coleman, S. & Roy, S. (2014). "Effect of Ultrasound on mass transfer during electrodeposition for electrodes separated by a narrow gap". *Elsevier, Journal of Chemical Engineering Science*, **11**, pp. 35-45.
- Collis, J., Manasseh, R. , Liovic, P., Tho, P. , Ooi, A. & Duran, K. P. (2009). "Cavitation microstreaming and stress fields created by microbubbles". *Elsevier Publishers, Journal of Ultrasonics*, **50**, pp. 273 - 279.
- Costello, S., Strusevich, N., Flynn, D., Kay, R.W., Patel, M.K., Bailey, C., Price, D., Bennet, M., Jones, A.C. & Desmulliez, M.P.Y. (2013). "Electrodeposition of copper into high aspect ratio PCB micro-via using megasonic agitation". *Springer Verlag, Journal of Microsystems Technology*, pp. 1-8.
- Cravotto, G., Gaudino, E.C. & Cintas, P. (2013). "On the mechanochemical activation by ultrasound". *Journal of Chemical Society Review*, **42**, pp. 7521 - 7535.
- Dini, J. W. (1993). *Electrodeposition: The Materials Science of Coatings and Substrates*, Noyes Publications, Germany, Berlin.
- Ebnesajjad, S. (2010). *Handbook of Adhesives and Surface Preparation: Technology, Applications and Manufacturing*, Elsevier Science.
- Erpelding, T.N., Hollman, K.W. & O'donnell, M. (2007). "Bubble-based acoustic radiation force using chirp insonation to reduce standing wave effects". *Journal of Ultrasound in Medicine and Biology*, **33**, pp. 263 - 269.
- Etter, P.C. (1995). *Underwater Acoustic Modeling: Principles, techniques and applications, Second Edition*, Taylor & Francis.
- Gale, G. W. & Busnaina, A. A. (1999). "Roles of Cavitation and Acoustic Streaming in Megasonic Cleaning". *Particulate Science and Technology: An International Journal*, **17**, pp. 229-238.

- 1
2
3 Garich, H., Gebhart, L., Taylor, E.J., Inman, M. & Mccrabb, H. (2007). "Development and Characterization
4 of Plating Cell Geometry for Printed Circuit Board and Packaging Applications". *Journal of The*
5 *Electrochemical Society*, **3**, pp. 1- 10.
- 6 Gurrum, S.P., Edwards, D.R., Marchand-Golder, T., Akiyama, J., Yokoya, S., Drouard, J & Dahan, F 2012.
7 Generic Thermal Analysis for Phone and Tablet Systems. *Electronic Components and Technology*
8 *Conference (ECTC), 2012 IEEE 62nd*. IEEE.
- 9 Hauptmann, M., Struyf, H., Gendt, S. D., Glorieux, C. & Brems, S. (2013). "Evaluation and interpretation of
10 bubble size distributions in pulsed megasonic fields". *Journal of Applied Physics*, **113**, pp. 1-17.
- 11 Hennig, M., Neumann, J., Wixforth, A., Radler, J. O. & Schneider, M. F. (2009). "Dynamic patterns in a
12 supported lipid bilayer driven by standing surface acoustic waves". *The Royal Society of Chemistry,*
13 *Lab on a Chip*, **9**, pp. 3050-3053.
- 14 Hoffelner, J., Landes, H. & Lerch, R. (2000). "Calculation of Acoustic Streaming Velocity and Radiation
15 Force Based on Finite Element Simulations of Nonlinear Wave Propagation". IEEE Ultrasonics
16 Symposium, 2000. IEEE, pp. 585 - 589.
- 17 Hyde, M.E. & Compton, R.G. (2002). "How Ultrasound influences the electrodeposition of metals". *Elsevier*
18 *Publishers, Journal of Electroanalytical Chemistry*, **531**, pp. 19 - 24.
- 19 Ipc 1999. IPC-A-600F. *Acceptability of Printed Boards*, IPC Association Connecting Electronics Industries.
20 Northbrook, IL 60062-6135:
- 21 Kaufmann, J. , Desmulliez, M.P.Y, Price, D., Hughes, M., Strusevich, N. & Bailey, C. "Influence of
22 megasonic agitation on the electrodeposition of high aspect ratio blind vias". 2nd Electronics
23 System integration Technology Conference, 2011 Greenwich, UK. IEEE, pp. 1235-1241.
- 24 Kaufmann, J.G., Desmulliez, M.P.Y., Tian, Y., Price, D., Hughes, M., Strusevich, N., Bailey, C., Liu, C. &
25 Hutt, D. (2009). "Megasonic agitation for enhanced electrodeposition of copper". *Springer,*
26 *Microsystems and Technology*, **15**, pp. 1245-1255.
- 27 Kocks, U.F., Tomé, C.N. & Wenk, H.R. (2000). *Texture and Anisotropy: Preferred Orientations in*
28 *Polycrystals and Their Effect on Materials Properties*, Cambridge University Press.
- 29 Lee, D. M., Folkerts, J. T., Collins, F. L., Dietrich, A. E. & Keeney, A. (2010). "Comparison of the
30 Electrochemical and Physical Properties of Nanocrystalline Copper Deposition in the Fabrication of
31 Printed Wiring Boards ". IPC APEX EXPO Technical Conference 2010 Las Vegas. IPC, pp. 492 -
32 451.
- 33 Lucke, T. & Beecham, S. (2009). "Cavitation, aeration and negative pressures in siphonic roof drainage
34 systems". *Building Serv. Eng. Res. Technol*, **30**, pp. 103-121.
- 35 Martin, S. (2013). *Sonocrystallization of Fats*, Springer.
- 36 Minzari, D., Grumsen, F.B., Jellesen, M.S., Moller, P. & Ambat, R. (2011). "Electrochemical migration of
37 tin in electronics and microstructure of the dendrites". *Elsevier, Journal of Corrosion Science*, **53**,
38 pp. 1659-1669.
- 39 Muller, S., Reuschel, T., Donadio, R.R., Kwark, Y.H., Bruns, H.D. & Schuster, C. (2015). "Energy-Aware
40 Signal Integrity Analysis for High-Speed PCB Links". *IEEE Transactions of Electromagnetic*
41 *Compatability*, **57**, pp. 1226 - 1234.
- 42 Okubo, T. , Shibaura, T.S., Hosoi, T., Tsuyoshi, H. & Mitsui, F.K. (2013). "Signal Transmission Loss on
43 Printed Circuit Borad in GHz Frequency Region". IEEE Electrical Design of Advanced Packaging
44 & Systems Symosium (EDAPS), 2013 Nara, Japan. IEEE, pp. 112 - 115.
- 45 Peiponen, K.E., Myllylä, R. & Priezhev, A.V. (2009). *Optical Measurement Techniques: Innovations for*
46 *Industry and the Life Sciences*, Springer.
- 47 Rienstra, S.W. & Hirschberg, A. (2013). *IWDE 92-06: An Introduction to Acoustics*, Publisher: Eindhoven
48 University of Technology.
- 49 Roelfs, B., Dambrowsky, N., Erben, C & Kenny, S. (2013). "Filling Through Holes and Blind Micro Vias
50 With Copper Using Reverse Pulse Plating And Insoluble Anodes". *Atotech*. Available at:
51 http://www.atotech.com/fileadmin/pdf/papers/el/Roelfs_Kenny_Through_hole_BMV_filling.pdf
52 (Accessed Accessed 18th April).
- 53 Schlesinger, M. & Paunovic, M. (2011). *Modern Electroplating*, Publisher: John Wiley & Sons, New Jersey,
54 USA.
- 55 Sivasankar, B. (2008). *Engineering Chemistry*, McGraw-Hill Education, New Delhi.
- 56
57
58
59
60

- 1
2
3 Strusevich, N., Desmulliez, M.P.Y., Abraham, E., Flynn, D., Jones, T., Patel, M. & Bailey, C. (2013).
4 "Electroplating for high aspect ratio vias in PCB manufacturing : enhancement capabilities of
5 acoustic streaming". *Springer Verlag, Journal of Advanced Manufacturing*, pp. 211-217.
- 6 Tang, S.C. & Clement, G.T (2009a). "Acoustic standing wave suppression using randomized phase-shift-
7 keying excitations (L)". *Journal of Acoustical Society of America*, **126**, pp. 1667 - 1671.
- 8 Tang, S.C. & Clement, G.T. (2009). "Standing wave suppression in transcranial ultrasound therapy using
9 random-signal-modulation excitation". *International Ultrasonics Symposium, 2009b. IEEE*, pp. 2048
10 - 2051.
- 11 Trelleborg. (2008). "Aerospace Engineering Guide". *Trelleborg Sealing Solutions*. Available at:
12 www.tss.trelleborg.com (Accessed 3 March 2016).
- 13 Verdan, S., Burato, G., Comet, M., Reinert, L. & Fuzellier, H. (2003). "Structural changes of metallic surface
14 induced by ultrasound". *Elsevier, Journal of Ultrasonics Sonochemistry*, **10**, pp. 291-295.
- 15 Verhaagen, B. & Fernández, R. D. (2016). "Measuring cavitation and its cleaning effect". *Ultrasonics -
16 Sonochemistry*, **29**, pp. 619-628.
- 17 Wang, J. & Y. Huang, T. Yu, S. Zhu, M. Shen, W. Li, J. Wang (2014). "The migration of Cu species over
18 Cu-SAPO-34 and its effect on NH3 oxidation at high temperature". *Journal of the Royal Society of
19 Chemistry, Catal. Sci. Technol*, **4**, pp. 3004-3012.
- 20 Yan, J.J., Chang, L.C., Lu, C.W. & Dow, W.P. (2013). "Effects of organic acids on through-hole filling by
21 copper electroplating". *Electrochimica Acta*, pp. 1 - 12.
- 22 Zhou, Y. & Gao, X. W. (2013). "Variations of bubble cavitation and temperature elevation during lesion
23 formation by high-intensity focused ultrasound". *Journal of Acoustical Society of America*, **132**, pp.
24 1683-1694.
- 25 Zygo. (2016), "NewViewTM 8000 Series". available at: <http://www.zygo.com/?/met/profilers/newview8000/>
26 (Accessed 1 March 2016).
27
28
29
30
31
32
33
34
35
36
37
38
39
40
41
42
43
44
45
46
47
48
49
50
51
52
53
54
55
56
57
58
59
60